Director
Dr. Grigori Astrakharchik
Departament de Física (FIB)

Màster oficial en

Modelització Computacional Atomística i Multiescala en Física, Química i Bioquímica

Treball Final de Màster

Simulació amb Monte Carlo quàntic d'experiments de bombament topològic en gasos ultrafreds unidimensionals.

Simulación con Monte Carlo cuántico de experimentos de bombeo topológico en gases ultrafríos unidimensionales.

Quantum Monte Carlo simulation of experiments on topological pumping in one-dimensional ultracold gases.

Alex Teruel Piñol

Juliol de 2022

UNIVERSITAT DE BARCELONA
B:KC Barcelona Knowledge Campus
Campus d'Excel·lència Internacional
UPC UNIVERSITAT POLITÈCNICA DE CATALUNYA BARCELONATECH

Títol: **Simulació amb Monte Carlo quàntic d'experiments de bombament topològic en gasos ultrafreds unidimensionals.**

Estudiant: Alex Teruel Piñol

Data: Juliol de 2022

Director: Dr. Grigori Astrakharchik
Departament de Física (FIB)

Els gasos de bosons en una dimensió són des de fa dècades un tema de gran interès des del punt de vista teòric i més recentment també han esdevingut molt populars entre els grups de recerca experimentals. A més, en els darrers anys l'interès pels sistemes topològics quàntics ha incrementat substancialment des de que l'any 2016 es guardonés amb el premi Nobel de física a David J. Thouless, F. Duncan M. Haldane i J. Michael Kosterlitz per l'ús de conceptes topològics en la descripció de la matèria exòtica. Per tal de generar aquest tipus de matèria, l'ús d'àtoms ultrafreds és altament avantatjós, ja que permet tenir un gran control sobre les interaccions i la geometria del sistema, així com un gran grau de puresa. És en aquest context que l'equip experimental de Benjamin Lev va aconseguir observar bombament topològic en un gas de bosons unidimensional, el qual va ser un gran avenç. Fins aleshores, s'havia aconseguit realitzar la transició d'un gas en règim Tonks-Girardeau (altament repulsiu) a super Tonks-Girardeau (altament atractiu) mitjançant una ressonància Feshbach, però no s'havien estudiat estats topològicament excitats en gasos unidimensionals. En aquest darrer experiment l'equip va aconseguir creuar la ressonància diversos cops, ajustant el camp magnètic en àtoms dipolars, i va observar nous estats topològicament excitats que no havien estat realitzats fins aleshores.

L'objectiu principal d'aquesta tesi és estudiar el bombeig topològic en gasos quàntics. Concretament, considerem un sistema unidimensional homogeni compost per bosons que interactuen mitjançant una suma de potencials de contacte i d'interacció dipol-dipol. Proporcionem un ansatz de Jastrow senzill per a l'estat fonamental i pels estats topològicament excitats. Mitjançant el mètode Montecarlo variacional calculem propietats estructurals i energètiques en funció de la densitat, la longitud de dispersió i la força i orientació dipolar. L'energia es confronta a les recents mesures realitzades pel grup de Benjamin Lev en gasos ultrafreds unidimensionals. Es troba un bon acord per a l'energia de l'estat fonamental per a valors arbitraris de la força d'interacció, que van des de les interaccions febles fins a les fortes. L'ansatz proposat descriu correctament l'energia dels estats topològicament excitats en el règim d'interaccions fortes, quan la longitud de dispersió és petita en comparació amb la distància mitjana entre partícules. A més de l'energia, estudiem les propietats estructurals. Prediem propietats interessants de la matriu de densitat a un cos, quantificant la pèrdua de coherència, i de la funció de distribució a parelles. Aquestes prediccions es poden verificar en futurs experiments amb gasos quàntics topològicament excitats.

Título: **Simulación con Monte Carlo cuántico de experimentos de bombeo topológico en gases ultrafríos unidimensionales.**

Estudiante: Alex Teruel Piñol

Fecha: Julio del 2022

Director: Dr. Grigori Astrakharchik
Departamento de Física (FIB)

Los gases de bosones unidimensionales son desde hace décadas un tema de gran interés desde el punto de vista teórico y más recientemente también se han vuelto muy populares entre los grupos de investigación experimentales. Además, en los últimos años el interés por los sistemas topológicos cuánticos ha incrementado sustancialmente desde que el año 2016 se galardonase con el premio Nobel de física a David J. Thouless, F. Duncan M. Haldane i J. Michael Kosterlitz por el uso de conceptos topológicos en la descripción de la materia exótica. Para generar este tipo de materia, el uso de átomos ultrafríos es muy ventajoso, ya que permite tener un gran control de las interacciones y la geometría del sistema, así como un gran grado de pureza. Es en este contexto que el grupo experimental de Benjamin Lev consiguió observar bombeo topológico en un gas de bosones unidimensional, lo cual fue un gran logro. Hasta entonces, se había conseguido realizar la transición de un gas en régimen Tonks-Girardeau (altamente repulsivo) a super Tonks-Girardeau (altamente atractivo) mediante una resonancia Feshbach, pero no se habían estudiado estados topológicamente excitados en gases unidimensionales. En este último experimento, el equipo consiguió cruzar la resonancia varias veces, ajustando el campo magnético en átomos dipolares, y observó nuevos estados topólogicamente excitados que no habían sido realizados hasta la fecha.

El principal objetivo de esta tesis es estudiar el bombeo topológico en gases cuánticos. Concretamente, consideramos un sistema unidimensional homogéneo compuesto por bosones que interactúan mediante una suma de potenciales de contacto y de interacción dipolo-dipolo. Proporcionamos un ansaz de Jastrow sencillo para el estado fundamental y para los estados topológicamente excitados. Mediante el método Montecarlo variacional calculamos propiedades estructurales y energéticas en función de la densidad, longitud de dispersión y fuerza y orientación dipolar. La energía se confronta a las recientes medidas realizadas por el grupo de Benjamin Lev en gases ultrafríos unidimensionales. Se encuentra un buen acuerdo para la energía del estado fundamental para valores arbitrarios de la fuerza de interacción, que van desde las débiles interacciones hasta las fuertes. El ansaz propuesto describe correctamente la energía de los estados topológicamente excitados en el régimen de interacciones fuertes, cuando la longitud de dispersión es pequeña en comparación con la distancia media entre partículas. Además de la energía, estudiamos sus propiedades estructurales. Predecimos propiedades interesantes de la matriz de densidad en un cuerpo, cuantificando la pérdida de coherencia, y de la función de distribución a parejas. Estas predicciones pueden verificarse en futuros experimentos con gases cuánticos topológicamente excitados.

Title: **Quantum Monte Carlo simulation of experiments on topological pumping in one-dimensional ultracold gases.**

Student: Alex Teruel Piñol

Date: July of 2022

Supervisor: Dr. Grigori Astrakharchik
Departament of Physics (FIB)

One-dimensional boson gases have been a field of great interest from a theoretical point of view for decades and more recently have also become very popular among experimental research groups. In addition, the appeal of quantum topological systems has increased substantially since the 2016 Nobel Prize in Physics was awarded to David J. Thouless, F. Duncan M. Haldane, and J. Michael Kosterlitz for the use of topological concepts in the description of exotic matter. In order to generate such a type of matter, the use of ultra-cold atoms is highly advantageous, as it allows a great control over the interactions and geometry of the system, as well as a high degree of purity. In that context, Benjamin Lev's experimental group was able to observe topological pumping in a one-dimensional boson gas, which was a very relevant recent achievement. Until then, the transition from a Tonks-Girardeau (highly repulsive) to a super Tonks-Girardeau (highly excited attractive) gas had been achieved by means of a Feshbach resonance, but topologically excited states have not been studied in one-dimensional gases. In this last experiment, the group was able to cross the resonance several times, by tuning the magnetic field in dipolar atoms, and observed new topologically excited states, which were not realized until then.

The main goal of the present thesis is to study topological pumping in quantum gases. Concretely, we consider a homogeneous one-dimensional system composed of bosons interacting via a sum of contact and dipole-dipole interaction potentials. We provide a simple Jastrow ansatz for the ground state and for topologically excited states. By using the variational Monte Carlo method we calculate structural and energetic properties as a function of the density, scattering length, dipolar strength and orientation. The energy is confronted with the recent measurements performed in Benjamin Lev's group in one-dimensional ultracold gases. A good agreement is found for the ground-state energy for arbitrary values of the interaction strength, ranging from weak to strong interactions. The proposed ansatz correctly describes the energy of the topologically excited states in the regime of strong interactions, when the scattering length is small compared to the mean interparticle distance. In addition to energy, we study structural properties. We predict interesting features in the one-body density matrix, quantifying the loss of coherence, and pair distribution function. Such predictions can be verified in future experiments with topologically excited quantum gases.

Prèviament a aquest treball, el grup de recerca (bàsicament el Dr. Astrakharchik és amb qui vaig tenir contacte) ja havia estudiat àmpliament el camp del gasos de bosons unidimensionals i per tant vaig poder enriquir-me de les publicacions disponibles i comprovar que els resultats que anava obtenint a mesura que avançàvem en el treball eren raonables. No obstant, el treball que vaig realitzar estava bastant enfocat al desenvolupament del codi que ens proporcionaria les prediccions pel sistema estudiat, per tant no vaig fer us de cap codi prèviament escrit i vaig partir de zero. A continuació anomeno les meves contribucions:

- Resoldre el problema de *scattering* fent servir com a funció d'ona una funció de Jastrow i utilitzant com a condicions de contorn (1) condicions periòdiques de contorn i (2) condicions de Bethe-Pierls. Aquesta part va consistir en un desenvolupament d'aquestes expressions que donava lloc a una equació sense solució analítica. Per aquesta equació vaig implementar un codi en FORTRAN que resolia el problema utilitzant el mètode de la bisecció. També vaig proposar una aproximació analítica al voltant d'un punt d'interès.
- Implementar una serie de subrutines en FORTRAN que calculessin els observables que ens interessaven, és a dir: energia cinètica, energia potencial deguda a les interaccions de contacte, energia local (cinètica + contacte), energia potencial dipolar, funció de distribució radial, matriu de densitat a un cos, factor d'estructura estàtic i distribució de moments. Aquesta serie de subrutines les vaig anar elaborant al llarg del projecte.
- Implementar una subrutina en FORTRAN que fent us de l'algorisme de Metropolis realitzes el *sampling* de les configuracions en el nostre codi MC.
- Implementar el programa Monte Carlo variacional (VMC) principal que fent ús de les subrutines que he comentat realitzés la simulació.
- Implementar una serie de *scripts* que s'encarreguessin de realitzar cada simulació fent servir diferents llavors inicial i que emmagatzemessin els resultats en fitxers de dades. També vaig implementar *scripts* per poder realitzar simulacions a llarg de rangs de densitats/longituds de *scattering*, els quals eren força útils per algunes etapes del treball.
- Implementar dos programes en FORTRAN que s'encarreguessin de realitzar el anàlisi estadístic de les dades. Un d'ells era per les energies i l'altre per les funcions de correlació.
- Quan el codi ja estava escrit vaig haver de fer una serie de verificacions per veure que tot funcionava correctament (testeig del codi).
- Amb el codi ja verificat vaig analitzar els diferents resultats obtinguts comparant-los amb diferents models existents.
- Finalment, probablement el resultat més rellevant, utilitzant el codi que havia escrit vaig comparar les prediccions del VMC amb les mesures d'un experiment recent i vaig verificar que el model funcionava bé (en el seu rang de validesa).

FORMATTED REPORT

Quantum Monte Carlo simulation of experiments on topological pumping in one-dimensional ultracold gases.

Author: Alex Teruel
Facultat de Física, Universitat de Barcelona, Diagonal 645, 08028 Barcelona, Spain.

Advisor: Grigori Astrakharchik.

Abstract: We consider a homogeneous one-dimensional system composed of bosons interacting via a sum of contact and dipole-dipole interaction potentials. We provide a simple Jastrow ansatz for the ground state and for topologically excited states. By using the variational Monte Carlo method we calculate structural and energetic properties as a function of the density, scattering length, dipolar strength and orientation. The energy is confronted with the recent measurements performed in Benjamin Lev's group in one-dimensional ultracold gases. A good agreement is found for the ground-state energy for arbitrary value of the interaction strength, ranging from weak to strong interactions. The proposed ansatz correctly describes the energy of the topologically excited states in regime of strong interactions, when the scattering length is small compared to the mean interparticle distance. In addition to the energy, we study structural properties. We predict interesting features in the one-body density matrix, quantifying the loss of coherence, and pair distribution function. Such predictions can be verified in future experiments with topologically excited quantum gases.

I. INTRODUCTION

The study of one-dimensional (1D) quantum gases has been a topic of high interest in the last decades and the fact that correlations and quantum fluctuations are magnified in low-dimensional systems makes them systems with great study possibilities, both from the theoretical and experimental points of view. An important topic is the study of the different regimes of one-dimensional quantum gases[1]. In most applications these systems the interaction potential can be described by a single parameter, the effective 1D scattering length a_{1D}, which is inversely proportional and opposite in sign to the coupling constant g_1D in one dimension. The one-dimensional Bose gas with zero-range interactions is known as a Lieb-Liniger[2] model for repulsive ($g_{1D} > 0$ and $a_{1D} < 0$) interactions and McGuire soliton[3] for attractive ones. Some of the energetic properties of these systems were obtained using the Bethe ansatz method in an exact way a dating back to 1960s [2, 4, 5]. More recent studies have focused on description of the correlation functions[6–8]. A particularly interesting limit is that of strongly repulsive interactions ($g_{1D} \to \infty$ and $a_{1D} \to 0^-$), called Tonks-Girardeau (TG) regime. In this case the gas of impenetrable bosons behaves as if it were compound of non-interacting spinless fermions as two particles cannot stay in the same place which remind the Fermi exclusion principle[9].However, if the resonant value of $g_{1D} = \infty$ is rapidly crossed the system still remains in a homogeneous gas-like state which no longer corresponds to the ground state but rather to a highly excited metastable state[10]. This new regime of strongly attractive interactions ($g_{1D} \to -\infty$ and $a_{1D} \to 0^+$) is called super Tonks-Girardeau (sTG) regime and is characterized by even stronger correlation as compared to the ones found in $g_{1D} \to \infty$ TG regime. The super Tonks-Girardeau regime has been observed in subsequent experiments [11].

Additionally, the interest in quantum topological systems has increased substantially since David J. Thouless, F. Duncan M. Haldane and J. Michael Kosterlitz were awarded with the Nobel Prize in 2016 for the use of topological concepts in the description of exotic matter. The fact that the use of ultracold atoms is very advantageous in the creation of exotic matter, due to the enhanced control that over the system properties, has made it a subject of great interest experimentally. In fact, in a recent experiment performed by Benjamin Lev group, topological pumping has been observed in a 1D Bose gas[12]. They used dysprosium atoms which have a large dipolar moment and enjoy a number of Feshbach resonances as the magnetic field is changed. As a result, the one-dimensional coupling constant as well crosses $g_{1D} = \text{inf}$ value several times. Physically, the obtained system is no longer described only by the value of g_{1D} but an additional integer number (topological index) is needed to describe system properties.

In this context, the aim of this project is to use a quantum Monte Carlo method to study 1D Bose gases along the resonance. Concretely, we have developed a variational Monte Carlo (VMC) code in FORTRAN 90 that calculates the energy of the system, pair distribution function, static structure factor, one-body density matrix (OBDM) and momentum distribution, using as a trial wave function a pair product of Jastrow functions. We have proposed to use the number of nodes of the Jastrow function as the topological property and modified the Lieb-Liniger Hamiltonian [2] by adding a dipole-dipole interaction (DDI) term [13, 14] as the Hamiltonian of the system. Our goal is to verify that the proposed topological parameter allows us to reproduce the different energy levels that have been observed experimentally and to see what effect the topological excitations have on the correlation functions.

II. MODEL HAMILTONIAN

A. General Problem

We study a system composed of N bosons that interact with each other through a sum of short-range and a dipolar interaction potentials. The short-range potential can be described by a contact pseudopotential

$$V_{sr}(r) = g_{3D}\delta(r)\frac{\partial}{\partial r}(r\cdot)\,, \tag{1}$$

where g_{3D} is the coupling constant related to the s-wave scattering length a_{3D} as $g_{3D} = 4\pi\hbar^2 a_{3D}/m$. The value of a_{3D} can be tuned by changing the magnetic field in the vicinity of a Feshbach resonance [15]. The dipole-dipole interaction (DDI) potential in three dimensions can be written as

$$V_{dd}(\vec{r}) = \frac{d^2}{r^3}(1 - 3\cos^2(\theta_{rd}))\,, \tag{2}$$

where $\vec{d}$ is the dipole moment, d^2 is the strength of the DDI and $\cos(\theta_{rd}) = \vec{r}\cdot\vec{d}/(rd)$. The angle θ_{rd} between particle pair, $\vec{r}$, and the orientation of the dipole, $\vec{d}$, can be changed in experiments[12]. In order to create 1D geometry, the bosons are confined by a cigar-shaped harmonic trap

$$V_{trap}(\vec{r}) = \frac{m}{2}[\omega_\parallel^2 x^2 + \omega_\perp^2(y^2+z^2)], \tag{3}$$

where $\omega_\parallel$ and $\omega_\perp$ are the trap frequencies of the axial and perpendicular directions. Thus, the full 3D Hamiltonian can be written as a sum of the kinetic, interaction and external potential energy,

$$\hat{H}_{3D} = \sum_i\left[-\frac{\hbar^2\nabla_i^2}{2m} + V_{trap}(\mathbf{r}_i)\right] + \sum_{i<j}[V_{sr}(\mathbf{r}_{ij}) + V_{dd}(\mathbf{r}_{ij})].$$

However, in presence of a tight transversal harmonic confinement, the wave function of each particle will have a Gaussian dependence on the transverse coordinates, y and z, according to $\exp[-1/(2a_\perp^2)(y^2+z^2)]$ where $a_\perp = \sqrt{\hbar/(m\omega_\perp)}$ is the oscillator width. In that case, the energy is dominated by the quantum fluctuations in the transverse confinement, $E \approx N\hbar\omega_\perp$. In the following, we consider only the motion along the longitudinal direction (x) and subtract the zero-point motion energy, $E_{1D} = E_{3D} - N\hbar\omega_\perp$.

B. One-Dimensional Problem

1. *Contact Interaction*

The scattering problem of two atoms in a wave guide ($\omega_\parallel = 0$) interacting via contact pseudopotential (1) can be reduced [16] to an effective 1D scattering with 1D contact interaction potential that can be approximated by the pseudo-potential

$$V_{sr}^{1D}(x) = g_{1D}\delta(x) = -\frac{2\hbar^2}{ma_{1D}}\delta(x), \tag{4}$$

where g_{1D} is the 1D coupling constant and a_{1D} the 1D s-wave scattering length. The 3D and 1D scattering lengths are related as $a_{1D} = -a_\perp(a_\perp/a_{3D} - C)$, where $C = 1.0326$ is a constant[16] arising from the summation over virtual excitations of the higher levels of the transverse confinement. This relation has a resonant behavior when $a_\perp$ is of the order of a_{3D}, i.e. $g \to \infty$, known as a Confinement Induced Resonance (CIR). Instead, C can be ignored for weak interactions ($a_{3D} \ll a_\perp$) where mean-field relation applies, $a_{1D} = -a_\perp^2/a_{3D}$. Therefore, the strength of 1D pseudopotential can be tuned by changing a_{3D} by means of the Feshbach resonance or by Confinement Induced Resonance via the strength of the transverse confinement. In our case we are not concerned with how experimentally the value of a_{1D} is adjusted, while keeping in mind that that a_{1D} can take any value. If we define the linear density of the gas as $n = N/L$, where N is the number of bosons and L the size of the system, then na_{1D} is the gas parameter and $\gamma = -2/(na_{1D})$ is the Lieb-Liniger parameter.

2. *Dipole-Dipole Interaction*

The effective 1D DDI potential can be obtained by integrating the 3D expression [Eq. (2)] along the y and z directions [13], [17], which results in

$$U_{DDI}^{1D}\left(\frac{|x|}{a_\perp}\right) = U_{dd}\tilde{V}_{dd}\left(\frac{|x|}{a_\perp}\right), \tag{5}$$

with the amplitude of the dipolar interaction given by

$$U_{dd} = -\frac{1}{8}\frac{d^2}{a_\perp^3}(1 + 3\cos(2\theta)), \tag{6}$$

and its shape defined by complementary error function $\mathrm{erfc}(x)$ according to

$$\tilde{V}'_{dd}(u) = -2u + \sqrt{2\pi}(1+u^2)e^{u^2/2}\,\mathrm{erfc}(u/\sqrt{2}). \tag{7}$$

In addition, there is a singular contribution which renormalizes the strength of the short-range potential, Eq. (9).

$$\tilde{V}_{dd}(u) = \tilde{V}'_{dd}(u) - \frac{8}{3}\delta(u), \tag{8}$$

It means, that for a repulsive extended 1D interaction potential (5), there is an additional attractive singular contribution,

$$V'^{\,1D}_{sr} = -\frac{8}{3}U_{dd}a_\perp\delta(x). \tag{9}$$

Figures (1, 2) show the strength and shape of the DDI potential. Positive, negative and zero values of U_{dd} define three characteristic regions in the range $\theta = 0 - 180°$ (and additional symmetric regions in the range $\theta = 180 - 360°$). The DDI is maximally repulsive at $\theta = 90°$ (side-to-side configuration) and maximally attractive at $\theta = 0°, 180°$ (head-to-tail configuration). Additionally, U_{dd} vanishes at $\theta \approx 55°, 125°$, so at those magic angles DDI is absent and δ-interacting gas is realized. If we look at the shape of DDI shown in Fig. (2), we observe a typical dipolar d^2/x^3 decay at large distances and a finite value at the origin.

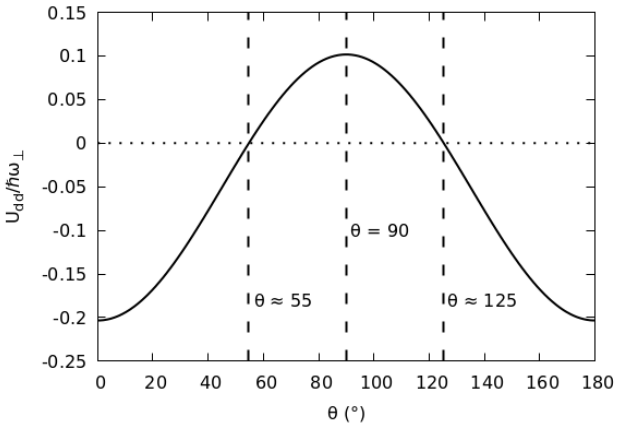

FIG. 1: Strength of the DDI U_{dd} as a function of the angle between particle pair and the orientation of the dipole θ, Eq. (12), using the typical experimental parameters values.

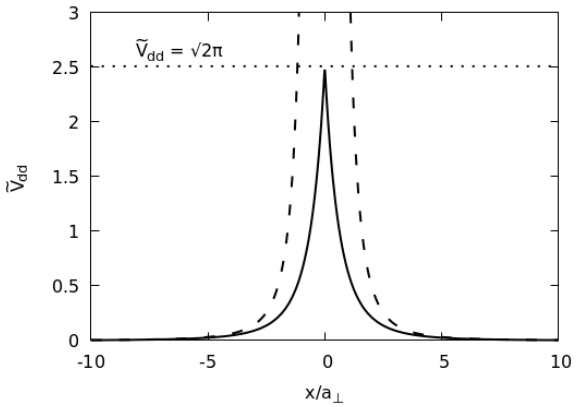

FIG. 2: Shape of the DDI $\tilde{V'}_{dd}$ as a function of the distance between particle pair (solid line), Eq. (7). The shape has an asymptotic tendency proportional to x^{-3} (dashed lines) for large values of x and a peak of $\sqrt{2\pi}$ at the origin (horizontal dotted line).

In order to make the Hamiltonian more compact, it is useful to group the singular contribution V'^{1D}_{sr} from the DDI with the contact interaction potential V^{1D}_{sr}, thus creating a new effective contact interaction potential with a new effective s-wave scattering length

$$a = \frac{a_\perp}{\frac{4}{3}\tilde{U}_{dd} + a_\perp/a_{1D}}, \tag{10}$$

with $\tilde{U}_{dd} = U_{dd}/(\hbar\omega_\perp)$. Note that when U_{dd} is 0 ($\theta \approx 55^o$) in Eq. (10), we recover the only contact interaction case, $a = a_{1D}$, and it is convenient to use a_{1D} or the inverse of linear density n^{-1} as length units.

3. *Dimensionless Hamiltonian*

In order to perform numerical simulation, it is important to define dimensionless units. We use $a_\perp$ as length unit and $\hbar\omega_\perp = \hbar^2/(ma_\perp^2)$ as the unit of energy. We define $u = x/a_\perp$ as the dimensionless distance, so that the dimensionless 1D Hamiltonian can be written as

$$\frac{\hat{H}_{1D}}{\hbar\omega_\perp} = -\frac{1}{2}\sum_{i=1}^{N}\frac{\partial^2}{\partial u_i^2} + \sum_{i<j}\left[\tilde{U}_{dd}\tilde{V'}_{dd}(u_{ij}) - \frac{2}{a/a_\perp}\delta(u_{ij})\right]. \tag{11}$$

The main parameters that characterize the gas are the dimensionless DDI strength $\tilde{U}_{dd}$, the dimensionless contact interaction strength $a/a_\perp$ and the dimensionless linear density $na_\perp$.

4. *Topological Index*

Although an important part of the physics of this problem is described by the 1D Hamiltonian, it is observed experimentally that for same values of the parameters described above, different energy values are obtained. Therefore, there must be an additional parameter that fully describes the system and allows us to predict the energies of the topologically excited states. In this work we call it the *topological index* ℓ, which will be formally introduced in section IV and allows us to find different energies for the same values of the parameters described in this section.

III. EXPERIMENTAL PARAMETERS

To verify that the results of the simulations are correct, it is convenient to use the values of the parameters that define our system from some experiment that has been realized. In experiments with quasi-one-dimensional dipolar gases, commonly, a 2D optical lattice with a lattice wave-length λ and a lattice depth E_R is used to realize the quasi-1D confinement, and the system is characterized by the transverse harmonic oscillator length $a_\perp$ and dipole length a_{dd}. The dipole length is related to the the strength of the DDI according to [18], $d^2 = \hbar^2 3a_{dd}/m$, so the dimensionless dipolar strength can be rewritten as

$$\tilde{U}_{dd} = -\frac{1}{8}\frac{3a_{dd}}{a_\perp}(1 + 3\cos(2\theta)). \tag{12}$$

For typical experimental parameters [12] one has $a_\perp = 952a_0$, $a_{dd} = 129a_0$, $m = 161.9267984m_a$, where a_0 is the Bohr radius and m_a the atomic mass. Thus, the dimensionless strength is $\tilde{U}_{dd} = -0.050814(1+3\cos(2\theta))$.

IV. MONTE CARLO IMPLEMENTATION

In order to find the energetic and structural properties of the system, we implemented a variational Monte Carlo code (VMC). This section explains the main parts of the implementation, however, the code itself is not shown. A brief description of VMC method is given in Section 2.1 in Ref. [19].

A. Trial Wave Function

In this implementation we used a trial wave function of Jastrow pair-product form

$$\psi(x_1, \cdots, x_N) = \prod_{i<j} f(x_{ij}). \tag{13}$$

Where $f(x)$ is Jastrow function and $x_{ij} = |x_i - x_j|$ with periodic boundary conditions (explained later),

$$f(x) = \cos(kx + \delta), \tag{14}$$

where k is the scattering momentum and δ the phase shift. The wave function can be rewritten as

$$\psi(x_1, \cdots, x_N) = \exp\left(\sum_{i<j} u_2(x_{ij})\right), \tag{15}$$

$$u_2(x) = \log(f(x)) = \log(\cos(kx + \delta)), \tag{16}$$

where $u_2(x)$ is the logarithmic Jastrow function. In VMC calculation, the square wave function is sampled to accept/reject new configurations (k') from an initial state (k). Concretely, it means that the movement $x_k \to x_{k'}$ is accepted with probability 1 when $\Delta u > 0$ and $\exp(2\Delta u)$ when $\Delta u < 0$ (Metropolis algorithm).

$$\Delta u = \sum_{i \neq k} [u_2(x_{ik'}) - u_2(x_{ik})]. \tag{17}$$

B. Simulation Box and Boundary Conditions

The simulations are done in a system of N particles confined in a 1D simulation box of length L. In order to minimize the finite size effects two boundary conditions are imposed: (i) Periodic Boundary Conditions

$$\psi(x_1..., x_i, ..., x_N) = \psi(x_1..., x_i + L, ..., x_N), \tag{18}$$

thus,

$$f'(L/2) = 0, \tag{19}$$

and (ii) for δ pseudopotential, Bethe-Pieirls boundary condition applies

$$\left.\frac{f'(x)}{f(x)}\right|_{x=0} = -\frac{1}{a}. \tag{20}$$

C. Two-Body Problem

When the boundary conditions are imposed on the Jastrow function (or its logarithmic version), the scattering momentum and the phase shift get fixed. Firstly, by imposing PBC, we find

$$k\frac{L}{2} + \delta = \ell\pi, \tag{21}$$

where ℓ is the topological index. Secondly, by imposing Bethe-Pieirls boundary condition, we find

$$\tan(\delta) = \frac{1}{ka}. \tag{22}$$

Finally, if we combine Eq. (21) and Eq. (22), the expression that fix δ for a given values of k and ℓ is

$$\frac{2a}{L}(\delta - \ell\pi) + \frac{1}{\tan(\delta)} = 0. \tag{23}$$

This equation does not have an analytic solution, but it is easy to see that δ lies between 0 and π, so an easy way to find its exact numerical value is by means of the dichotomy method. An alternative way to find the solution analytically by doing a Taylor expansion around the region of strongly attractive/repulsive gases ($a \to 0$). In this limit, δ can be approximated by $\pi/2 + \Delta\delta$, with $\Delta\delta \to 0$. Thus, $cot(\delta) \approx -\Delta\delta - \Delta\delta^3/3 + O(4)$, and substituting this expression in Eq. (23) we obtain

$$\Delta\delta^3 + 3\left(\frac{2a}{L} + 1\right)\Delta\delta + \frac{6a\pi}{L}\left(\ell - \frac{1}{2}\right) = 0, \tag{24}$$

which has always one solution when $a > -L/2$. This expression could be used to find solutions around $a = 0$, however, in this study we do not explore this way. In Fig. (3) there is a comparison of both methods. It can be seen that the results obtained from the analytical expression are reasonable close to zero, but the discrepancy increases rapidly with a_{1D}.

In Eq. (21) the topological index ℓ is introduced, which is related with the number of nodes in the Jastrow term. Concretely, in the attractive regime ($g_{1D} < 0$) ℓ is exactly the number of nodes and in the repulsive regime ($g_{1D} > 0$) ℓ is equal to the number of nodes minus one, as we can see in Fig. (5), where nodes position is plotted as a function of a_{1D}. Additionally, Fig. (4) the profile of

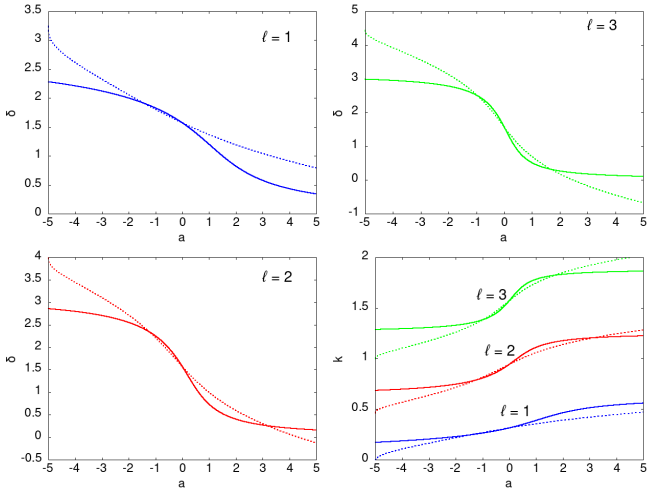

FIG. 3: Scattering momentum k and phase shift δ obtained from numerical solution of Eq. (23) (solid lines) and analytical solution of Eq. (24) (dashed lines) as function of the s-wave scattering length a. Box length $L = 10$ and topological index $\ell = 1, 2, 3$ (blue, red, green).

$f(x)$ for different values of the 1D s-wave scattering wave length with $\ell = 1$. When $a_{1D} = 0$, (impenetrable gas) there is a node at $x = 0$ and the gas has a similar behavior than an ideal Fermi gas, which allows us to compare some of the results with the analytical expressions of it. We can also observe that for $a_{1D} < 0$ there are no nodes, which means that the gas is in the ground state. However, when $a_{1D} > 0$ (attractive gas) there is always one node and the gas is in an exited state. When $a_{1D} \to -\infty$, there are no nodes, $f(x)$ is constant and the system behaves as an ideal Bose gas.

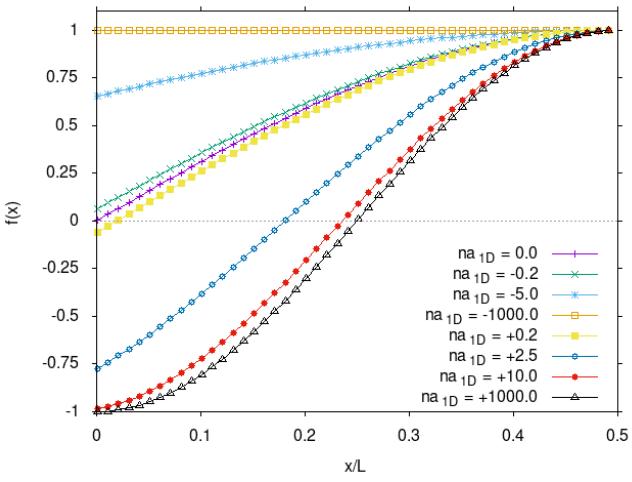

FIG. 4: Jastrow function using different s-wave scattering length and with topological index $\ell = 1$, one (zero) node in the attractive (repulsive) regime.

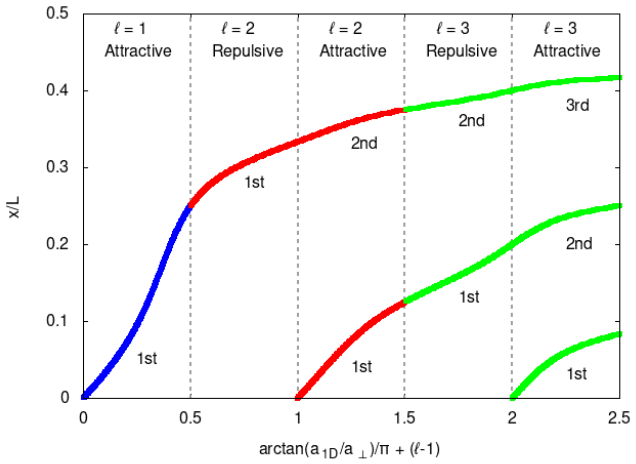

FIG. 5: Evolution of node position (vertical axis) as function of 1D scattering length a_{1D} (horizontal axis) and topological index $\ell = 1, 2, 3$ (blue, red, green). Vertical dashed lines separate the different regions, which go from $a_{1D} \to -\infty$ to $a_{1D} \to \infty$.

D. Observables

In this section we introduce energetic and structural quantities of interest. Mainly, we are interested in finding the total energy of the quantum system, which is the sum of the kinetic, short-range interaction and dipole-dipole interaction energies. There are different ways to compute the energy, but in this implementation we calculate all the local contributions (kinetic and short range) together and then we add the DDI ($E = E_{loc} + E_{DDI}$). From the definitions in Section II, it can be shown that the local contributions can be calculated by

$$E_{loc} = -\frac{\hbar^2}{2m}\left\langle \sum_{i=1}^{N} F_i^2 + \sum_{j\neq i} \frac{d^2u_2}{dx^2}\bigg|_{x_{ij}} \right\rangle, \tag{25}$$

where $F_i = \sum_{j>i} (du_2/dx)|_{x_{ij}} (x_i - x_j)/x_{ij}$ is the drift force. To compute the DDI contribution, we only have to add the contribution of each pair of particles,

$$E_{DDI} = \left\langle \sum_{i<j} U_{dd}\tilde{V}'_{dd}\left(\frac{|x_{ij}|}{a_\perp}\right) \right\rangle . \tag{26}$$

Additionally, we have calculated the correlation functions $g_1(x)$ and $g_2(x)$ and their Fourier transforms $n(k)$ and $S(k)$. The one-body density matrix and pair distribution function are defined as

$$g_1(x) = \frac{N}{n}\frac{\int \psi^*(x_1 + x, x_2, ..., x_N)\psi(x_1, ..., x_N)dx_2...dx_N}{\int |\psi(x_1, ..., x_N)|^2 dx_1...dx_N}, \tag{27}$$

$$g_2(x_{12}) = \frac{N(N-1)}{n^2}\frac{\int |\psi(x_1, ..., x_N)|^2 dx_3...dx_N}{\int |\psi(x_1, ..., x_N)|^2 dx_1...dx_N}. \tag{28}$$

In practise, the pair distribution function $g_2(x)$ quantifies the probability of finding two particles (i and j) separated by distance $x = x_i - x_j$ and can be calculated by doing a histogram of $x_i - x_j$. The one-body density matrix $g_1(x - x')$ measures the coherence in the system and is related to probability of inserting a particle at position x' once it was destroyed at position x. To compute $g_1(x)$ we calculate the histogram of $\exp(\Delta u(x))$, where x is $x'_k - x_k$ in Eq. (17). Momentum distribution $n(k)dk$ counts number of particles having momentum between k and $k + dk$ and can be obtained from OBDM by a Fourier transform

$$n(k) = n \int \exp(ikx) g_1(x) dx, \tag{29}$$

where $k = 2\pi j/L$ are allowed momenta with $j = 0, 1, \cdots$. The static structure factor is related via Fourier transform

$$S(k) = 1 + n \int \exp(ikx)(g_1(x) - 1) dx \tag{30}$$

to the pair distribution function and quantifies the diagonal correlations in the system. In particular, in a crystal the peak in $S(k)$ is macroscopic and proportional to the total number of particles N. The height of momentum distribution $n(k)$ with $k \to 0$ quantifies off-diagonal long-range order and is proportional to N if Bose-Einstein condensation occurs.

V. RESULTS

A. Code Testing

In this section we demonstrate that the code works properly. To do so, the results obtained from simulations of an impenetrable gas ($a_{1D} = 0$), with $\ell = 1$ and $U_{dd} = 0$, are compared with the analytical solution. In this case, the parameters of Jastrow function are $k = \pi/L$ and $\delta = \pi/2$, so the bosonic wave function is the absolute value of ideal Fermi gas (IFG) wave function. Thus, the energy obtained from MC simulations can be compared with IFG energy, $(E/N)^{IFG} = \pi^2\hbar^2 n^2/(6m)\left(1 - 1/N^2\right)$, where term $(1 - 1/N^2)$ accounts for the finite size of the simulation box. Additionally, local properties such as pair distribution function and the static structure factor can be compared to IFG results, ${g_2}^{IFG}(x) = 1 - \mathrm{sinc}^2(\pi n x)$. Figures (6-8) show the results of the simulations as compared to the analytical expressions. It can be observed the results obtained from MC simulations reproduce the analytical expressions with great precision. In Fig. (6) is shown that the energy of an impenetrable gas has a quadratic dependence with the density and increases monotonically. This behaviour is exactly the same that we expect of an IFG. The fact that $g_{1D} \to \infty$ for an impenetrable gas produces a similar efect to the Pauli exclusion principle

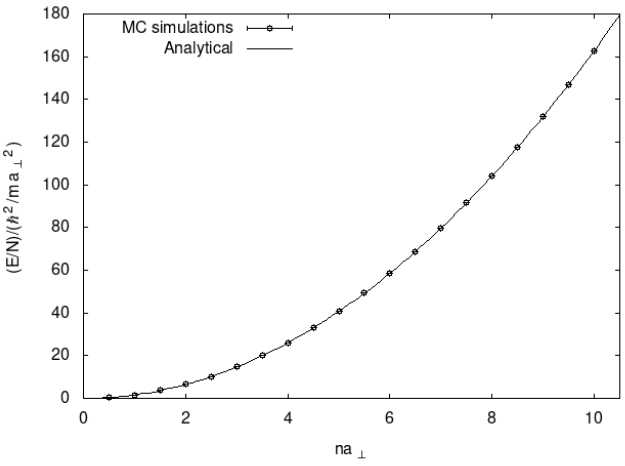

FIG. 6: Equation of state (EoS) of an impenetrable gas obtained from MC simulations (circles) compared to analytical solution of an IFG (solid line).

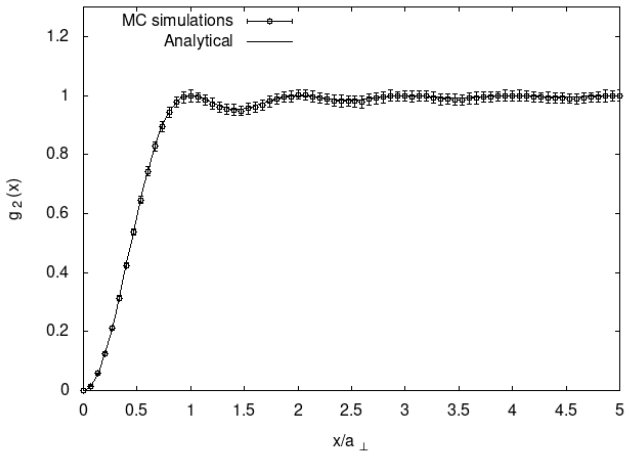

FIG. 7: Pair distribution function of an impenetrable gas obtained from MC simulations (circles) compared to analytical result of an IFG (solid line).

for fermions. That is, in both cases two particles cannot be in the same position, as it can be seen in Fig. (8), where the value of $g_(x)$ in the origin is 0. When x increases, Friedel oscillations are shown. In the static structure factor, Fig. (8), a clear kink appears at $2k_F$, where $kF = \hbar\pi n/m$ is the Fermi momentum of the associated Fermi gas.

B. Strongly attractive/repulsive regimes

In this Section we analyse the correlation functions and energy of the system for ground and topologically excited states in the regime of strong interactions, when the scattering length a_{1D} is small compared to the mean

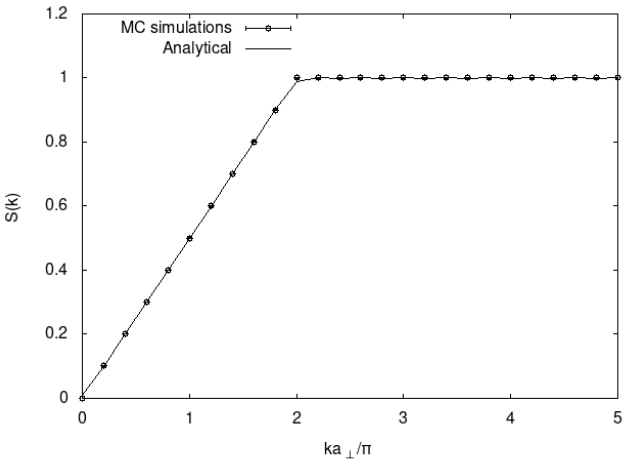

FIG. 8: Static structure factor of an impenetrable gas obtained from MC simulations (circles) compared to analytical result of an IFG (solid line).

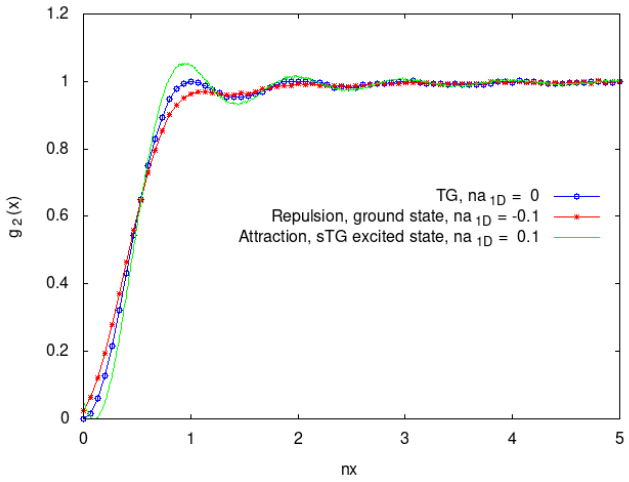

FIG. 9: Pair distribution function for characteristic values of scattering length a_{1D} and topological index $\ell = 1$. (blue circles) Tonks-Girardeau (IFG) gas; (red circles) ground state in repulsive gas; (green line) excited state in attractive gas.

interparticle distance, $n\,|a_{1D}| \ll 1$.

1. *Gas with short-range interactions and $\ell = 1$*

In Fig. (9) we show the pair distribution function for three characteristic values of the 1D scattering length a_{1D}. In the repulsive case, $a_{1D} < 0$, there is no node, which is consistent with the fact that the wave function has no nodes. Additionally, the fact that $g_2(x)$ is not zero at the origin implies that two particles can be at the same position and the system can collapse. It is also observable that $g_2(x) < 1$ for all values of x. On the other hand, if we look at the attractive case, we see that there is a finite value at the origin and a node near the origin, which describes a highly excited state. The correlations are higher than in the other cases, which is deduced from a higher peak on $g_2(x)$.

In Fig. (10) the one-body density matrix is represented. It can be seen that $g_1(x)$ decreases faster (coherence loss is faster) in the excited case, $a_{1D} > 0$, as compared to the the rest. However, for large distances (from $nx \gtrsim 2$) their behavior is similar. In fact, Luttinger liquid theory [20] predicts asymptotic long-range power-law behavior of the one-body density matrix according to [21]

$$g_1(x) \propto \left(\frac{1}{nd(x,L)}\right)^{\frac{1}{2K}}, \tag{31}$$

where K is the Luttinger parameter and $d(x,L)$ is the chord distance, which is the length of a "chord" that joins two points of a circumference of length L.

$$d(x,L) = \frac{L}{\pi}\sin\left(\frac{\pi x}{L}\right) \tag{32}$$

Due to the fact that we are working with PBCs, the distance between two points that we obtain from the simulations is actually the length of the arc that joins the two points of a circumference of perimeter L. As a result, the finite-size effects become evident at the edges of the box, compare blue and black lines in Fig. 10. To correct this we use $d(x,L)$ instead of x and if we look at Fig. (11) we see that effectively for large distances a power law is fulfilled. By means of an adjustment we have found that the value of the Luttinger parameter is similar to $K \approx 1$, which is the value that the theory predicts for a Tonks-Girardeau gas.

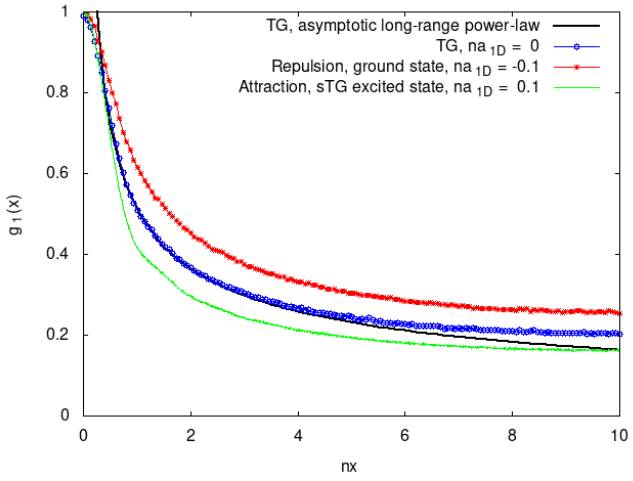

FIG. 10: OBDM for characteristic values of scattering length a_{1D} and topological index $\ell = 1$. (blue circles) Tonks-Girardeau (IFG) gas; (red circles) ground state in repulsive gas; (green line) excited state in attractive gas; (black solid line) asymptotic long-range behaviour of TG gas.

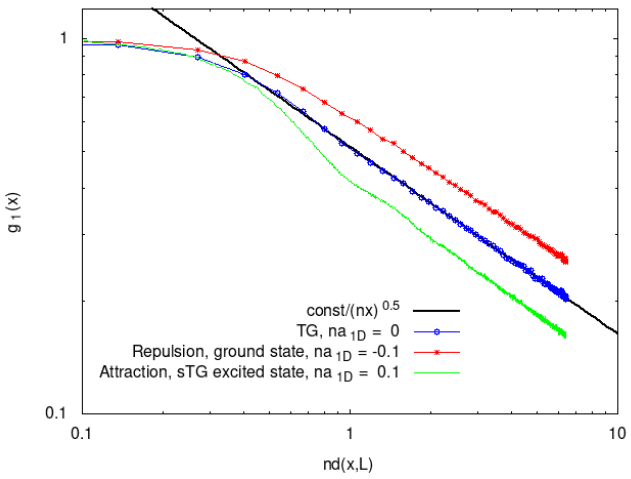

FIG. 11: OBDM for characteristic values of scattering length a_{1D} and topological index $\ell = 1$. (blue circles) Tonks-Girardeau (IFG) gas; (red circles) ground state in repulsive gas; (green line) excited state in attractive gas. Asymptotic long range power-law (black solid line) is fitted to the data and $K \approx 1$ is obtained. The axes are in logarithmic scale and the distance is corrected using Eq. (32).

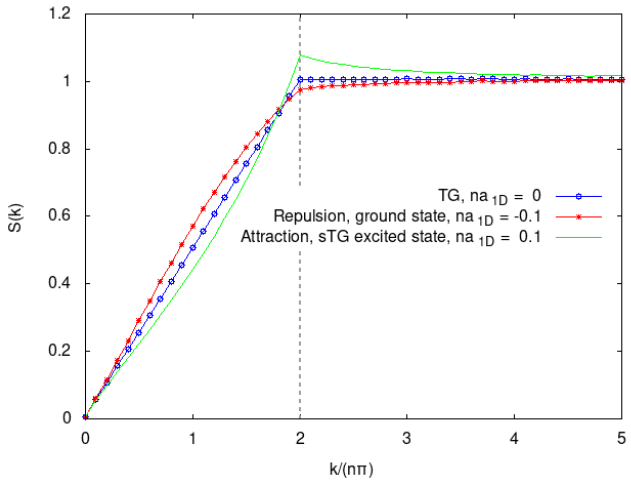

FIG. 12: Static structure factor for characteristic values of scattering length a_{1D} and topological index $\ell = 1$. (blue circles) Tonks-Girardeau (IFG) gas; (red circles) ground state in repulsive gas; (green line) excited state in attractive gas. Vertical dashed line shows the position of twice the Fermi wave vector.

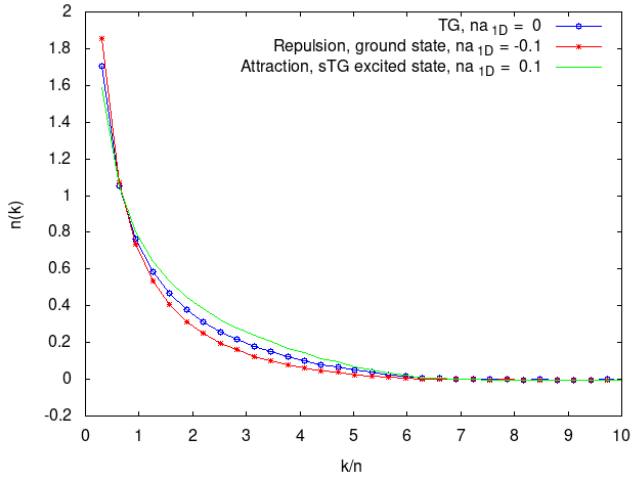

FIG. 13: Momentum distribution for characteristic values of scattering length a_{1D} and topological index $\ell = 1$. (blue circles) Tonks-Girardeau (IFG) gas; (red circles) ground state in repulsive gas; (green line) excited state in attractive gas.

Figure (12) shows the static structure factor. In all three cases we observe that $S(k)$ linearly increases from 0 according to linear phonon relation, $S(k) = \hbar|k|/(2mc)$, where c is the speed of sound, and the value of the Luttinger parameter $K \equiv v_F/c$ can be extracted according to $S(k) = (1/2)K|k|/k_F$. For large momenta, $S(k)$ tends to the uncorrelated value $S(k) = 1$. However, the shapes are a qualitatively different in the special point $k = 2kF$. In the ground-state repulsive case there is no peak and $S(k)$ smoothly increases. In the TG case, a kink is formed at a special point, $k = 2k_F$, related to the *umklapp* process in the ideal Fermi gas in which a particle is taken from Fermi sphere $k_1 = k_F$ and is promoted to the opposite side of the Fermi sphere, $k_2 = -k_F$, which changes the momentum by $k_1 - k_2 = 2k_F$ but carries no energy change. In the excited attractive case, a peak is formed at $k = 2k_F$ followed by a slow decay to $S(k) = 1$.

The momentum distribution shown in Fig. (13) presents a peak when $k \to 0$ for all cases. The kinetic energy can be calculated from it as $E_{kin}/N = \int_{-\infty}^{\infty} \hbar^2k^2/(2m)\ n(k)dk/(2\pi)$. In order to have E_{kin} finite, the asymptotic $|k| \to \infty$ value must be $n(k) \to 0$ which is correctly reproduced. In principle, $n(k)$ is expected to satisfy a $1/k^4$ decay for large momenta, but the relative error of our simulations when k increases is too large as $n(k) \to 0$ which corresponds to very small values of $n(k)$ making verification of the power-law behavior complicated. Figure 14 reports the occupation of the Bose Einstein condensate quantified by $n(k)$ with the smallest allowed momentum. For all values of a_1D we find that the height of the peak at small momentum always grows as the number of particles N is increased, signaling a divergence at $k = 0$ in the thermodynamic limit. A macroscopic occupation of the zero-momentum state, $n(k = 0) \propto N$, would be a manifestation of a true Bose-Einstein condensate (BEC). Instead, in the one-dimensional case, we observe that the height of the peak is proportional to $N^{1/2}$, which is a reminiscence of condensation [6].

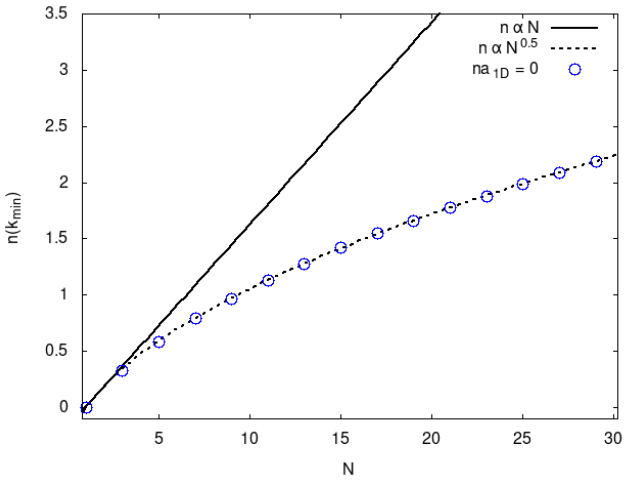

FIG. 14: Occupation of the Bose Einstein condensate inferred from the height of the momentum distribution peak at $k_{min} = 2\pi/L$ as function of the number of particles for an impenetrable gas (blue circles). The solid line shows a lineal tendency and the dotted line a square root tendency.

2. *Dipolar gas with $\ell = 1$*

Although we have not observed significant differences in the correlation functions when introducing the DDI, differences can be observed in the equation of state depending on the specific value of θ used. The reason why correlation functions are not strongly affected by the DDI is because for small values of a, i.e. strong short-range interaction, the pseudopotential provides the dominant contribution and as we rely on plane-wave ansatz for the trial wave function.

Equations of state are shown in Figs. (15, 16) for repulsive ($a_{1D}/a_\perp = -0.1$) and attractive ($a_{1D}/a_\perp = 0.1$) short-range interactions with $\ell = 1$ and different values of dipole orientation θ. Dipolar interactions are maximally repulsive for $\theta = 90°$, maximally attractive for $\theta = 0°$ and vanishing at the magic angle $\theta \approx 55°$. In addition, we plot the equation of state of an which has a quadratic dependence and an EoS of a gas of hard rods (HR),

$$\left(\frac{E}{N}\right)^{HR} = \frac{\pi^2}{6(1-na_{1D})^2}\frac{\hbar^2 n^2}{m}, \tag{33}$$

which is obtained from IFG energy by taking into account the excluded volume correction, $L \to \text{Ł} - Na_{1D}$.

In the repulsive case, shown in Fig. 15, we observe that the energy per particle increases monotonically and that the equation of state of a HR gas predicts very well the energy in the range $na_{1D} \leq 0.25$ without DDI ($\theta \approx 55°$). In the excited attractive case, shown in Fig. 16, the energy per particle does not increase monotonically but instead reaches a maximum at $na_\perp \approx 4.6$ ($na_{1D} \approx 0.46$). In this case the equation of state of a HR gas fits well for smaller values of the gas parameter, $na_{1D} \leq 0.1$. In both cases the effect of DDI ($\theta = 0°$ and $\theta = 90°$) is small for low densities (practically the same energy) and increases with the density. When $\theta = 0°$, the DDI is attractive ($U_{dd} < 0$) and the energy per particle decreases. On the contrary, when $\theta = 90°$, the DDI is repulsive and the energy increase.

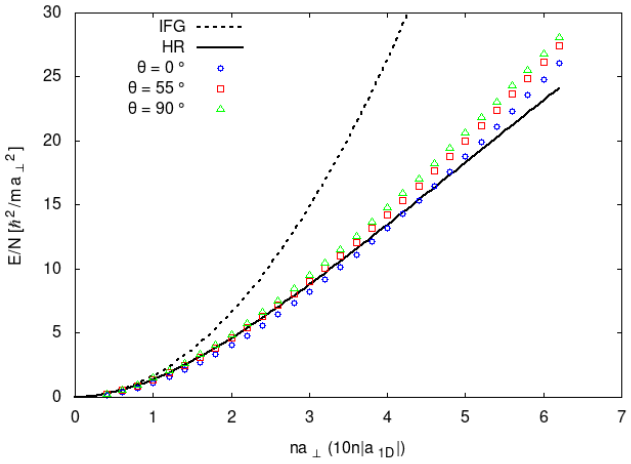

FIG. 15: Energy per particle of a repulsive gas ($a_{1D}/a_\perp = -0.1$) with $\ell = 1$ as function of the density for different values of the angle between the pair of particles and the dipole θ. Circles, squares and triangles ($\theta = 0°, 55°, 90°$) show the results obtained from MC simulations. The dashed line shows the equation of state of an IFG and the solid line of a HR.

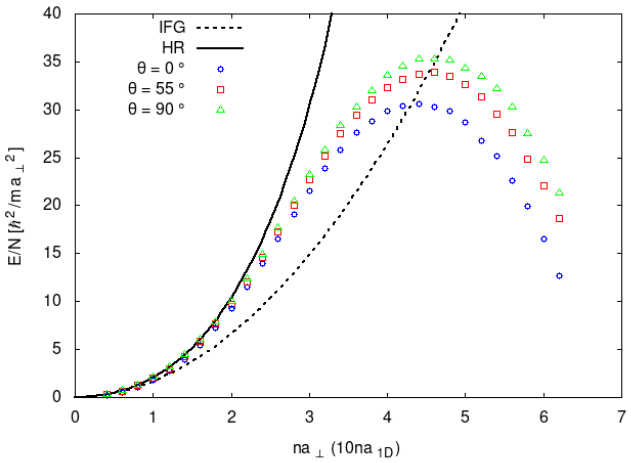

FIG. 16: Energy per particle of an attractive gas ($a_{1D}/a_\perp = 0.1$) with $\ell = 1$ as function of the density for different values of the angle between the pair of particles and the dipole θ. Circles, squares and triangles ($\theta = 0, 55, 90$) show the results obtained from MC simulations. The dashed line shows the equation of state of an IFG and the solid line of a HR.

3. *Gas with short-range interactions and $\ell = 2$*

In the following we show the results obtained for topologically excited states with $\ell = 2$. In Fig. (17) we represent the Jastrow functions of the repulsive, impenetrable and attractive cases. We can observe that the gas in repulsive regime has one node, that is it describes an excited state, whereas the other two have two nodes, corresponding to a topologically double excited states. Furthermore, it can be observed that the second node of impenetrable and attractive cases and the node of repulsive case are very close to $x/L \approx 1/3$. Due to this fact, the pair distribution functions present a valley at $x/L \approx 1/3$, which means that it is highly improbable to find two particles at that distance. Finally, Fig. (19) shows the one-body density matrix in which a peak gets formed at the same distance as the valley of $g_2(x)$. If we interpret $g_1(x)$ as the probability of removing a particle from $x_0 = 0$ and generating another at x, then this result seems reasonable because $nx \approx 6.66$ is the region where it is least likely to find a particle and, consequently, where it is easier to put a new particle.

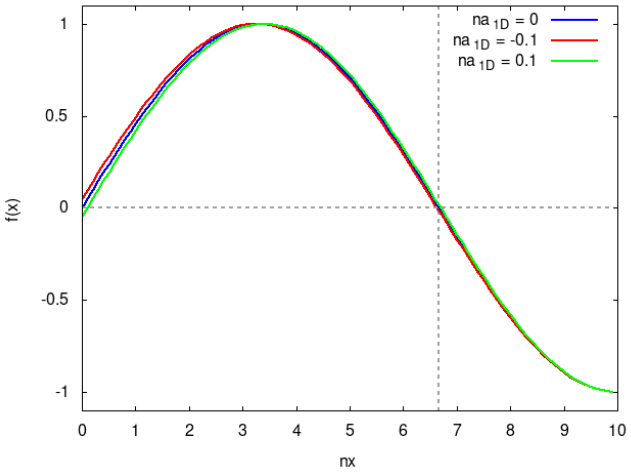

FIG. 17: Jastrow functions of gases with a gas parameter $na_{1D} = 0, -0.1, 0.1$ (blue, red, green) and topological index $\ell = 2$. The three wave functions share a node close to $x/L = 1/3$ (that is $nx \approx 6.67$ for $N = 20$), shown with a vertical dotted line.

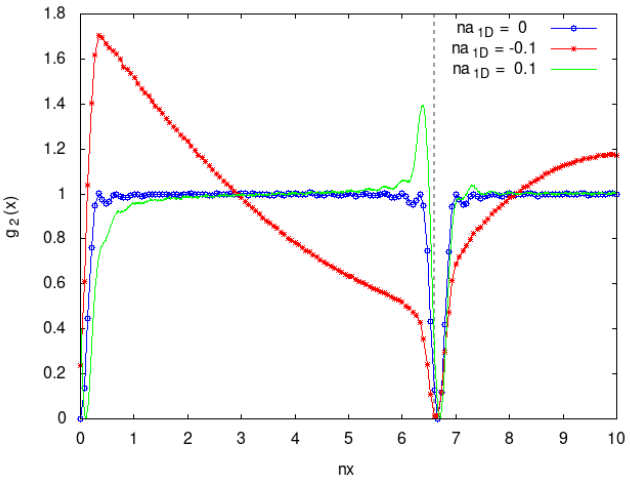

FIG. 18: Pair distribution function of gases with a gas parameter $na_{1D} = 0, -0.1, 0.1$ (blue, red, green) and topological index $\ell = 2$. The three functions present a valley near $nx \approx 6.66$ (vertical dotted line) which coincides with the nodes of Jastrow functions.

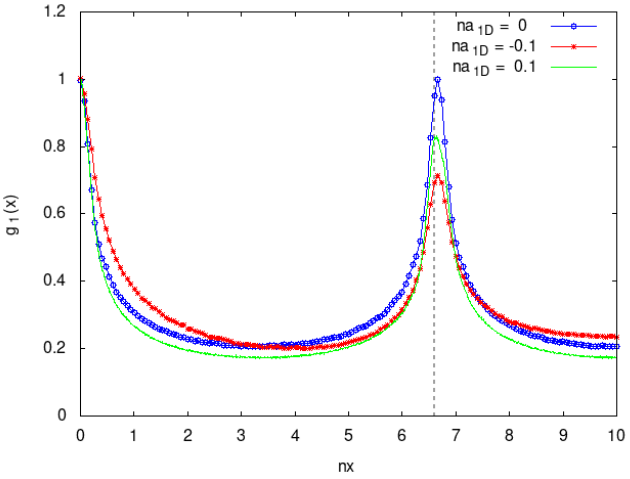

FIG. 19: One-body density matrix of gases with a gas parameter $na_{1D} = 0, -0.1, 0.1$ (blue, red, green) and topological index $\ell = 2$. The three functions present a peak near $nx \approx 6.66$ (vertical dotted line) which coincides with the nodes of Jastrow functions and the valleys of pair distribution functions.

C. Comparison with experiments

In this Section we present the most important result, which is a comparison of VMC energy with the energy measured in experiments with ultracold 1D gases in Benjamin Lev's group[12]. To do this comparison we ran simulations for a wide range of $a_{1D}/a_\perp$ with a fixed linear density $na_\perp = 1$. Experiments used $N = 20 - 30$ particles and we fix the number of particles to $N = 20$. Each simulation was done using 50 different initial seeds of the random generator and averaging the results. The obtained energy is shown in Fig. (20), where the grey circles (blue squares) are the energy per particle experimentally measured in the repulsive (attractive) regime. The red dotted and green solid lines are the energy obtained from VMC calculations in repulsive and attractive regimes. The error bars of the statistical error obtained from simulations are not shown and are smaller than the symbol size. It can be observed that VMC predictions provide very good agreement with the experimental data

in the ground state, $\ell = 1$ and $a_{1D} < 0$ (lower red dotted line) for all values of a_{1D}. For topologically excited stat with $\ell = 1$ and $a_{1D} > 0$ (lower green solid line), the VMC results a reasonable agreement with experimental data for $\gamma \gtrsim 10$. However, for smaller values of γ the VMC energy falls down and does not reproduce the experimental data in $n|a_{1D}| \gtrsim 0.2$ regime, not captured by our simple choice for the trial wave function. The upper red line ($\ell = 2$ and $a_{1D} < 0$) fits well the experimental data for $na_{1D} \leq 0.1$ ($\gamma \gtrsim 20$), but for larger values of the gas parameter na_{1D}, we exit the region of applicability of our trial wave function and the energy per particle is underestimated. Green line shows the case with a double topological excitation ($\ell = 2$ and $a_{1D} > 0$) and it shows a good agreement with experimental data for $na_{1D} \leq 0.1$ ($\gamma \gtrsim 20$). Therefore, the VMC approach predicts well the energy for all values of scattering length in the ground state ($a_{1D} < 0$ when $\ell = 1$) and for excited states in the regime of strong interactions ($n|a_{1D}| \leq 0.1$ when $\ell > 1$).

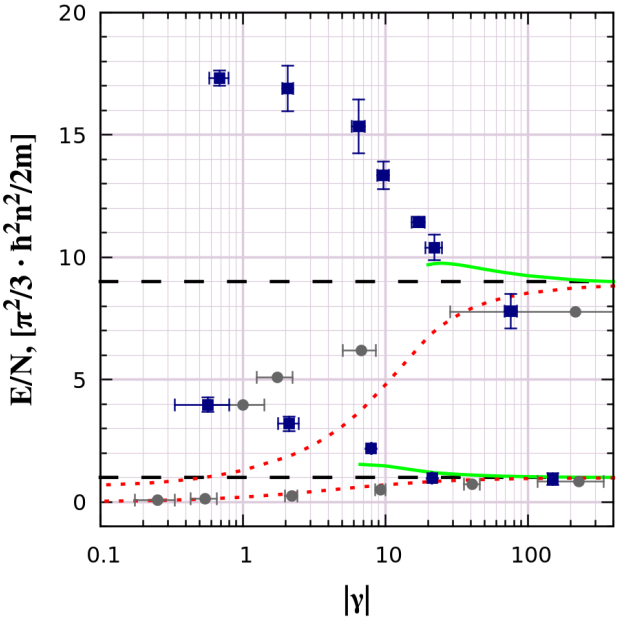

FIG. 20: Energy per particle as a function of the absolute value of Lieb-Liniger parameter $|\gamma|$. The grey circles (blue squares) are the experimental data of energy per particle in the repulsive (attractive) regime. The red dotted lines show the VMC results in ground state ($\ell = 1$) and excited state ($\ell = 2$) repulsive regime ($a_{1D} < 0$) in ascending order. The green solid lines show the VMC results in single excited state ($\ell = 1$) and double excited state ($\ell = 2$) attractive regime ($a_{1D} > 0$) in ascending order.

VI. CONCLUSIONS

In conclusion, we have studied a system of 1D bosons interacting simultaneously via a contact and a dipolar interaction by developing a VMC code using a Jastrow function as a trial function. This has allowed us to analyze energetic and structural properties. We have analyzed the pair distribution function both in the ground state and in excited states. For excited states we have found valleys for for the repulsive and attractive cases which coincide with one third of the box length. We have also studied the one-body density matrix, where we have verified that for large distances a power law decay is observed, in agreement with predictions of the Luttinger liquid theory. We have also found that for excited states a peak appears in the one-body density matrix, which position coincides with the valleys in the pair distribution function. Regarding the static structure factor, a different behavior is observed around $k = 2k_F$ point. In the repulsive ground state it follows a monotonous behavior, a kink is formed for resonant $g_{1D} \to \infty$ ($a_{1D} = 0$) case, and a peak appears in the super Tonks-Girardeau regime. In the momentum distribution we observe a peak at the origin $k = 0$ that tends to infinity as the number of particles is increased. The height of this peak provides the occupation of the Bose Einstein condensate and we had found that it increases sub-linearly with the number of particles, thus no true Bose Einstein condensation occurs. Finally, the main result, we have compared the energies obtained in experiments [12] with our results and we have found that the proposed simple Jastrow ansatz correctly predicts the energy of the ground state for any value of the scattering length. Furthermore, we have confirmed that the number of nodes in the Jastrow wave function is related to the the topological index ℓ and allows one to explore the topologically excited states of the system. By comparing the energy for excited states we have confirmed that our ansatz correctly predicts this energy when the scattering length is small compared to the mean interparticle distance ($n|a_{1D}| \leq 0.1$). For larger values a contribution from the ground-state is admixed and our ansatz underestimates the energy of the excited state and our simple Jastrow ansatz is no longer applicable.

As a future task, it would possible to improve the quality of the plane-waves Jastrow terms by solving numerically the two-body scattering problem with the dipolar interaction potential. This would allow to get a better variational description and will allow calculation of the equation of state of the gas using different values of the angle between pairs of particles and the direction of the dipole θ. Thus, from these equations of state it will be possible to fit an analytical expression for the chemical potential μ as a function of the gas parameter na_{1D} for different values of θ. Then, making use of the local density approximation (LDA) explained in [22] and the fitted parameters, it is possible to calculate a quantity known as frequency of the breathing mode as a function of another

quantity called LDA characteristic parameter. These two quantities are the ones represented in Fig. 2 in Ref. [12] for different values of θ. Therefore, by combining our VMC and LDA, we could make a comparison with the experiments for the frequency of the breathing mode.

Acknowledgments

I am not exaggerating when I say that the study of quantum gases is a non-trivial task, there is a lot of new information that must be taken into account and, in occasions, it can be a bit overwhelming. That is why I would like to thank Dr. Grigori Astrakharchik for providing me with all the necessary information during the realization of this project, as well as periodic meetings, where we have followed step by step the plan that we defined at the beginning of the project.

Last but not least, I would like to thank my family for supporting me and my classmates for the collaboration that we have all had throughout this stressful but extremely interesting course.

[1] D. S. Petrov, G. V. Shlyapnikov, and J. T. M. Walraven, Phys. Rev. Lett. **85**, 3745 (2000), URL https://link.aps.org/doi/10.1103/PhysRevLett.85.3745.

[2] E. H. Lieb and W. Liniger, Phys. Rev. **130**, 1605 (1963), URL https://link.aps.org/doi/10.1103/PhysRev.130.1605.

[3] M. Beau, S. M. Pittman, G. E. Astrakharchik, and A. del Campo, Phys. Rev. Lett. **125**, 220602 (2020), URL https://link.aps.org/doi/10.1103/PhysRevLett.125.220602.

[4] E. H. Lieb, Phys. Rev. **130**, 1616 (1963), URL https://link.aps.org/doi/10.1103/PhysRev.130.1616.

[5] C. N. Yang and C. P. Yang, Journal of Mathematical Physics **10**, 1115 (1969), URL https://doi.org/10.1063%2F1.1664947.

[6] H. G. Vaidya and C. A. Tracy, Phys. Rev. Lett. **42**, 3 (1979), URL https://link.aps.org/doi/10.1103/PhysRevLett.42.3.

[7] D. M. Gangardt, Journal of Physics A: Mathematical and General **37**, 9335 (2004), URL https://doi.org/10.1088/0305-4470/37/40/002.

[8] G. Astrakharchik and S. Giorgini, Journal of Physics B: Atomic, Molecular and Optical Physics **39** (2005).

[9] M. Girardeau, Journal of Mathematical Physics **1**, 516 (1960), URL https://doi.org/10.1063%2F1.1703687.

[10] G. E. Astrakharchik, J. Boronat, J. Casulleras, and S. Giorgini, Physical Review Letters **95** (2005), URL https://doi.org/10.1103%2Fphysrevlett.95.190407.

[11] E. Haller, M. Gustavsson, M. J. Mark, J. G. Danzl, R. Hart, G. Pupillo, and H.-C. Nägerl, Science **325**, 1224 (2009), URL https://doi.org/10.1126%2Fscience.1175850.

[12] W. Kao, K.-Y. Li, K.-Y. Lin, S. Gopalakrishnan, and B. L. Lev, Science **371**, 296 (2021), URL https://doi.org/10.1126/science.abb4928.

[13] F. Deuretzbacher, J. C. Cremon, and S. M. Reimann, Phys. Rev. A **81**, 063616 (2010), URL https://link.aps.org/doi/10.1103/PhysRevA.81.063616.

[14] S. Giovanazzi and D. H. J. O?Dell, The European Physical Journal D **31**, 439 (2004), URL https://doi.org/10.1140%2Fepjd%2Fe2004-00146-7.

[15] H. Feshbach, Annals of Physics **5**, 357 (1958), URL https://doi.org/10.1016/0003-4916(58)90007-1.

[16] M. Olshanii, Phys. Rev. Lett. **81**, 938 (1998), URL https://link.aps.org/doi/10.1103/PhysRevLett.81.938.

[17] F. Deuretzbacher, J. C. Cremon, and S. M. Reimann, Phys. Rev. A **87**, 039903 (2013), URL https://link.aps.org/doi/10.1103/PhysRevA.87.039903.

[18] T. Lahaye, C. Menotti, L. Santos, M. Lewenstein, and T. Pfau, Reports on Progress in Physics **72**, 126401 (2009), URL https://doi.org/10.1088/0034-4885/72/12/126401.

[19] R. J. Needs, M. D. Towler, N. D. Drummond, and P. L. Ríos, Journal of Physics: Condensed Matter **22**, 023201 (2009), URL https://doi.org/10.1088/0953-8984/22/2/023201.

[20] F. D. M. Haldane, Phys. Rev. Lett. **47**, 1840 (1981), URL https://link.aps.org/doi/10.1103/PhysRevLett.47.1840.

[21] M. A. Cazalilla, Journal of Physics B: Atomic, Molecular and Optical Physics **37**, S1 (2004), URL https://doi.org/10.1088/0953-4075/37/7/051.

[22] G. E. Astrakharchik, Phys. Rev. A **72**, 063620 (2005), URL https://link.aps.org/doi/10.1103/PhysRevA.72.063620.